MODELING OF COAXIAL HELICOPTER FLIGHT CHARACTERISTICS

V. A. Anikin, B. A. Vassiliev, V.N.Kvokov
Kamov Company, Russia

Abstract

Main aspects of a coaxial helicopter flight characteristics analysis method, its main features and correlations of analytical and experimental data are presented.

Russia is the largest producer and operator of coaxial design helicopters. Though in Russia a lot of research is being carried out in the field of coaxial helicopter aerodynamics, occasional translations and publications about it appearing in the West are rather limited, as Mr. Coleman of Ames research center has once noted.

The present paper deals with modeling of aerodynamics and flight characteristics of coaxial helicopters. It contains a brief survey of publications available in this field that have appeared in Russia and analysis of current investigations carried out at Kamov Company.

Before the beginning of 1980-ties evaluation of coaxial rotor helicopters flight characteristics was mainly based on equivalent single rotor theory and classical theory of Glauert-Lokk further developed in Russia by B. N. Youriev, A. N. Mikhaylov and M. L. Mil. Coaxial rotors were replaced with a single rotor of double solidity (B. N. Youriev, L. S. Vildgrube, V. N. Shaidakov, G. N. Kvasha). Leading Kamov research engineers L. N. Potashnik and E. A. Petrosian brought these theories to a level of practical engineering application. Empirical "coaxiality" coefficients κ_{co} were introduced into design formulas for coaxial main rotors and an empirical coefficient κ_{st} was introduced to evaluate the main rotor downwash angles near the stabilizer. These coefficients depended upon flying conditions (horizontal flight, climb, descent etc.) and were "tuned" to a specific helicopter model. Inductive velocity distribution over the main rotor disk was considered to be constant or laterally variable according to the triangle law (with Pain type gradient).

Specific nature of coaxial rotor aerodynamics and, in particular, complexity of modeling inductive interaction between the rotors restrained the development of the coaxial rotor aerodynamics theory for a long period of time. So, a transition from equivalent rotor theory to coaxial rotor combination theory took place only in the 1970-ties with the surge of a linear disk vortex theory (V. A. Anikin) and a linear blade vortex theory (V. S. Vozhdaev and, later, B. N. Bourtsev). After that coaxial rotor aerodynamics investigations based on a nonlinear vortex theory started (S. M. Belotserkovsky's school).

Increase of helicopter airspeeds, disk loads and power-to-weight ratio required new approaches to the problem of coaxial helicopter flight performance analysis. Fig. 1 presents conditions of two closely positioned coaxial rotors operation with one rotor operating in the downwash of the other and airframe carrying elements (wing, stabilizer, keel) conditions of operation

These conditions are essentially different and vary depending upon the flying conditions. The airframe elements can get into different zones of the main rotor system downwash and their aerodynamic characteristics can essentially affect the coaxial helicopter performance through its balance. In this connection solution of a coaxial helicopter performance analysis task must be undertaken with consideration of the aircraft spatial balance based on solution of an inductive interaction task posed both for the rotors and for the rotors and the airframe. With the purpose of solving these tasks a coaxial rotors disk vortex theory was once developed that served the basis for development of a method and a program for coaxial rotors and coaxial rotor helicopter aerodynamic characteristic analysis [1]. A rich experience in application of such programs for practical task solution has been gained at Kamov Company (V. N. Kvokov, B.A. Vassiliev).

Formulation of Task

A steady helicopter motion in a combined system of coordinates is investigated. The c. g. motion is examined in a system of velocity coordinates and the helicopter rotation around the c. g. is examined in a body axis coordinate system. Spatial balance equations are obtained from known equations of motion. Longitudinal motion with coaxial rotors torque balance is examined, i.e.

$$(1)\quad \begin{aligned} &X_{CR} + X_{PL} + G\sin И = 0,\\ &Y_{CR} + Y_{PL} - G\cos И = 0,\\ &Mz_{CR} + Mz_{PL} = 0,\\ &M^{UP}_{Y\ CR} + M^{LO}_{Y\ CR} = M_{Y\ PL}. \end{aligned}$$

where:

CR – stands for coaxial rotor system

PL – stand for the airframe

Let us introduce indices «UP» for the upper and «LO» for the lower rotor.

Solution of system (1) gives helicopter attitude parameters, controls for attaining this attitude and power required. Solution (1) is based on a pattern of successive approximations and is connected with multiple appeals to analysis of the main rotor system aerodynamic characteristics. This is a labor consuming part of the method. So a procedure is developed that allows to reduce the number of such appeals to the minimum.

Based on A. N. Mikhaylov rotor theory in a system of velocity coordinates, solution of control collective pitch φ_o and rotor attack angle α_{MR} definition task that ensures specified propulsive $X_0 = -X_{PL} - G\sin И$ and lifting $Y_0 = G\cos И - Y_{PL}$ forces does no depend upon the rotors cyclic control. The values of $_{PL}$ and $У_{PL}$ themselves depend upon the solution of this task because the airframe and its elements angles of attack vary both under the effect of longitudinal control and inductive flow wash. However, the variations are not large: in the domain of operational angles of attack $_{PL}(\alpha)$ changes very little and $У_{PL}(\alpha)$value equals to 5…15% of the gross flying weight. As a result, with successful zero approximation of X_0 and Y_0 we obtain a nearly exact solution (1) with a minimum number of appeals to balance of forces.

From the equation of longitudinal moment

$$M_Z(д_Z) = M_{Z_{CR}}(д_Z = 0) + M^{д_Z}_{Z_{CR}} д_Z + M_{Z_{PL}} = 0$$

we can define a δ_z equivalent force longitudinal deflection angle without recapitulation of the main rotor system parameters.

In case of a coaxial design helicopter rotor differential pitch angle $Дφ_{CR}$ required for directional balancing is defined from the last equation (1).

Main rotor system aerodynamic characteristics

The disk vortex theory is used to define coaxial rotors aerodynamic characteristics including their inductive interaction. Let us first describe definition of inductive velocity properties and specific algorithmic applications for formulas [3,4,5].

Inductive velocities. Let us examine a k-bladed right rotor placed in a uniform steady flow. Let us put axes of the right coordinate system into the rotor enter so that axis **y** is perpendicular to the plane of rotation and directed upwards and axis **x** is directed to the flow. The rotor rotates around **y** axis at a rate of ω.

A vortex model is built as follows. The blade is schematically presented as a radial segment of the lifting line with circulation Γ that is constant with respect to radius ρ and azimuth θ. A continuous vortex sheet shed from the blades at velocity V forms a spatial washed screw shaped plane of constant pitch. The vortex column axis forms angle α with the rotor plane. When the vortex column goes down from the rotor $\alpha<0$.

Let us find an inductive velocity value in an arbitrary spatial point $\{x., y., z.\}$ and write its coordinates using the values of a polar radius value and azimuth angle ψ calculated from the negative half-axis **ox** in direction of the rotor rotation

$$(2) \qquad x_* = -r\cos\psi, \quad y_* = y, \quad z_* = r\sin\psi .$$

Let us use relative coordinates and mark them with an upper dash. The linear dimensions will refer to rotor radius R, velocities - to ωR and circulation - to к ωR^2. The vortex surface S equation set in a coordinate form

$$(3) \qquad \begin{aligned} \bar{o} &= -\bar{v}\cos б - \bar{c}\cos(И - ϑ), \\ \bar{з} &= \bar{v}ϑ\sin б, \quad \bar{ж} = \bar{c}\sin(И - ϑ), \end{aligned}$$

can be substituted together with (2) into Bio-Savare equation and we can pass to time averaged inductive velocities. As a result we get:

$$(4) \qquad \bar{υ}_{ai} = \frac{k}{4p\bar{V}}\int_0^1 \frac{d\bar{Γ}(\bar{ρ})}{d\bar{ρ}} I_{ai}(\bar{c}, \bar{r}, \bar{y}, ψ, \bar{V}, б)d\bar{c},$$

$$i = 1,2,3, \quad a_1 = x, a_2 = y, a_3 = z,$$

where

$$I_X = \frac{1}{2\pi}\int_0^{2\pi} \frac{\bar{c}\cos И(L\sin б - \bar{y}) + \bar{V}L_Z\sin б}{\left(L^* + L_X\cos б\right)} dИ,$$

$$I_Y = \frac{1}{2\pi}\int_0^{2\pi} [\frac{\bar{c}\cos И\cos\alpha}{L^* + L_X\cos б} + \frac{\bar{c}^2 - \bar{c}\bar{r}\cos(И - ψ) + \bar{V}L_Z\cos б}{L\left(L^* + L_X\cos б\right)}] dИ$$

$$I_Z = \frac{1}{2\pi}\int_0^{2\pi} \frac{-\bar{c}\sin И(L\sin б - \bar{y}) + \bar{V}\left(\bar{y}\cos б + L_X\sin б\right)}{L\left(L^* + L_X\cos б\right)} dИ$$

$$L = \sqrt{\bar{y}^2 + l^2}, \quad l = \sqrt{\bar{c}^2 + \bar{r}^2 - 2\bar{c}\bar{r}\cos(И - ш)},$$

$$L_x = \bar{ρ}\cos Θ - \bar{r}\cos ψ, \quad L_Z = \bar{ρ}\sin Θ - \bar{r}\sin ψ,$$

$$L^* = L - \bar{y}\sin б$$

Functions I_{ai} are effect functions reflecting inductive interaction of the rotor vortex structure of singular intensity in point (1). For a time average inductive

velocity value caused in point (2) by lifting lines (vortex bottom) we obtain:

$$\bar{x}_x = -\bar{x}_\phi \sin ш, \quad \bar{x}_z = -\bar{x}_\phi \cos ш,$$

where

$$\bar{x}_\phi = \frac{k\bar{y}}{4p}\int_0^1 \frac{d\bar{\Gamma}}{dc}\left\{\frac{1}{\pi}\int_0^\pi \frac{\cos(И - ш)dИ}{\left[\bar{y}^2 + 1^2\right]^{3/2}}\right\}d\bar{c}$$

The integral in brackets can be presented through ecliptic integrals

$$\{\ \} = \frac{2}{\pi k^2\left[\bar{y}^2 + (\bar{c} + \bar{r})^2\right]^{3/2}}\left[\frac{2 - k^2}{1 - k^2}E(k) + K(k)\right],$$

where

$$k^2 = \frac{4\bar{c}\,\bar{r}}{(\bar{c} + \bar{r})^2 + \bar{y}^2}$$

Numeric realization of formulas (4) is complicated by certain singularities in sub-integral expressions. It can be eliminated if we use Fourier series expansion [3,4]. Let us present the inductive velocity components as:

$$(5)\quad \bar{x}_{ai}(\bar{r},\bar{y},ш) = \bar{x}_r^{ai}(\bar{r},\bar{y}) + \sum_{n=1}^{\infty}\left[\bar{x}_{cn}^{ai}(\bar{r},\bar{y})\cos nш + \bar{x}_{sn}^{ai}(\bar{r},\bar{y})\sin nш\right]$$

$$i = 1,2,3,$$

where

$$\bar{x}_r^{ai} = \frac{k}{4\pi\bar{V}}\int_0^1 \frac{d\bar{\Gamma}}{d\bar{c}}I_r^{ai}d\bar{c}, \qquad \bar{x}_{cn}^{ai} = \frac{k}{4\pi\bar{V}}\int_0^1 \frac{d\bar{\Gamma}}{d\bar{c}}I_{cn}^{ai}d\bar{c}$$

$$\bar{x}_{sn}^{ai} = \frac{k}{4\pi\bar{V}}\int_0^1 \frac{d\bar{\Gamma}}{d\bar{c}}I_{sn}^{ai}d\bar{c}, \qquad I_r^{ai} = \frac{1}{2\pi}\int_0^{2\pi} I_{ai}dш$$

$$I_{cn}^{ai} = \frac{1}{\pi}\int_0^{2\pi} I_{ai}\cos n\psi dш, \quad I_{sn}^{ai} = \frac{1}{\pi}\int_0^{2\pi} I_{ai}\sin n\psi dш,$$

$$a_1 = x, a_2 = y, a_3 = z,$$

Let us integrate in (5), introduce new variables $\tilde{c} = \bar{c}/\bar{r}$, $\tilde{y} = \bar{y}/\bar{r}$, and let the wave go further. Then

$$\bar{x}_r^x = \frac{k}{4\pi\bar{V}}\int_0^1 \frac{d\bar{\Gamma}}{d\bar{c}}R^x d\bar{c}, \qquad \bar{x}_r^z = \frac{k}{4\pi\bar{r}}\int_0^1 \frac{d\bar{\Gamma}}{d\bar{c}}R^z d\bar{c},$$

$$\bar{x}_r^y = \frac{k}{4\pi\bar{V}}\int_0^1 \frac{d\bar{\Gamma}}{d\bar{c}}R^y d\bar{c}, \qquad \bar{x}_{sn}^x = \frac{k}{4\pi\bar{r}}\int_0^1 \frac{d\bar{\Gamma}}{d\bar{c}}Sn^x d\bar{c},$$

$$\bar{x}_{cn}^x = \frac{k}{4\pi\bar{V}}\int_0^1 \frac{d\bar{\Gamma}}{d\bar{c}}Cn^x d\bar{c}, \qquad \bar{x}_{sn}^y = \frac{k}{4\pi\bar{r}}\int_0^1 \frac{d\bar{\Gamma}}{d\bar{c}}Sn^y d\bar{c},$$

$$\bar{x}_{cn}^y = \frac{k}{4\pi\bar{V}}\int_0^1 \frac{d\bar{\Gamma}}{d\bar{c}}Cn^y d\bar{c}, \qquad \bar{x}_{cn}^z = \frac{k}{4\pi\bar{r}}\int_0^1 \frac{d\bar{\Gamma}}{d\bar{c}}Cn^z d\bar{c},$$

$$\bar{x}_{sn}^z = \frac{k}{4\pi\bar{V}}\int_0^1 \frac{d\bar{\Gamma}}{d\bar{c}}Sn^z d\bar{c},$$

Kernels R, S_n, C_n are harmonic components of effect functions. Let us introduce typical integrals

$$(6)\quad \begin{aligned} M_n &= (-1)^{n+1}\frac{2}{\pi}\int_0^\pi \frac{\cos n\varphi}{L}W_n d\Theta \\ N_n &= (-1)^n\frac{2}{\pi}\int_0^\pi \cos n\varphi W_n d\Theta \\ M_n^i &= (-1)^{n+1}\frac{2}{\pi}\int_0^\pi \frac{i\cos n\varphi}{L}W_n d\Theta \\ N_n^i &= (-1)^n\frac{2}{\pi}\int_0^\pi i\cos n\varphi W_n d\Theta \end{aligned}$$

Now kernels R, S_n, C_n can be written as

$$(7)\quad \begin{aligned} &S_n^x = tg\alpha M_n, \quad S_n^x = M_n, \\ &Sn^z = \frac{1}{2}\left(M_{n-1}^i - M_{n+1}^i\right) + \frac{\sin б\, N_n + yM_n}{\cos б}, \\ &C_n^x = \frac{1}{2}\left(M_{n-1}^i + M_{n+1}^i\right) - \frac{y\sin б\, M_n^i + N_n^i}{\cos б}, \\ &C_n^y = -yM_n^i + \frac{1}{2\cos б}\times \\ &\times\left[M_{n-1} - M_{n+1} + \sin б\left(M_{n+1}^i + M_{n-1}^i\right)\right], \\ &C_n^z = \frac{M_n^i}{\cos б}, \\ &R^x = \frac{1}{2}\left(C_0^x + S_0^z\right), \quad R^z = \frac{1}{2}\left(C_0^z - S_0^x\right), \\ &R^y = 1 - \frac{y}{2}M_0^i + \frac{1}{2\cos б}\left(M_1 + \sin\alpha M_1^i\right), \end{aligned}$$

where

$$W_n = \left[\frac{L}{1}\left(1 + \frac{iy}{L}\right)\frac{\cos б}{1 + \sin б}\right]^n,$$

$$\sin\varphi = \frac{c\sin И}{l},\quad \cos\varphi = \frac{c\cos И - 1}{l},$$

$$l = \sqrt{c^2 + 1 - 2c\cos И}\ ,\ L = \sqrt{l^2 + y^2}\ ,$$

$$i = \begin{cases} 1, & L\sin б > y \\ -1, & L\sin б \le y \end{cases},$$

Formulas (7) contain an extracted singularity in sub-integral expressions. It is described by function $i(\Theta, \rho, y, \alpha)$, that shows a 1st order discontinuity at the border of the vortex cylinder. From the function properties it follows that the whole space is divided into two parts: in the first sub-space function $i(\Theta)=const$ retains its sign at $\Theta\in[0,\pi]$ and in the second sub-space it shows a discontinuity at $\Theta_* = \arg\left(L(\Theta)\sin\alpha = y\right)$, point but retains a constant value in domains $\left[(0, И_*)\cup(И_*, \pi)\right]$.

Let us examine a number of cases [5]

Case E – calculation of inductive velocity in disk plane y=0. Here

$$i^E = \mathrm{sgn}(б),\qquad i^E\sin б = |\sin б|,$$

$$W_n^E = \left[\frac{\cos б}{1+|\sin б|}\right]^n = W_n^E(б),$$

(8)

$$M_n^E = (-1)^{n+1} W_n^E(б)\frac{\pi}{2}\int_0^{\pi}\frac{\cos n\varphi}{l}dИ,$$

$$N_n^E = (-1)^n W_n^E(б)\frac{\pi}{2}\int_0^{\pi}\cos n\varphi dИ,$$

and we get $(-1)^n W_n^E(б) = к_б^n$, where $к_б^n$ is defined in [6]

$$S_n^x = \mathrm{tg}б\, M_n^E,\ S_n^y = M_n^E,$$

$$S_n^z = \frac{i^E}{2}\left[\left(M_{n-1}^E - M_{n+1}^E\right) + 2\mathrm{tg}б\, N_n^E\right],$$

$$C_n^x = -\frac{i^E}{2}\left[\left(M_{n-1}^E + M_{n+1}^E\right) + \frac{2}{\cos б}N_n^E\right],$$

(9)

$$C_n^y = \frac{1}{2}\left(M_{n+1}^E\frac{1}{W_1^E(б)} - M_{n-1}^E W_1^E(б)\right),$$

$$C_n^z = \frac{i^E}{\cos б}M_n^E,\ R^x = -\frac{i^E\cos б}{1+|\sin б|}д_0(c),$$

$$R^y = д_0(c),\qquad R^z = -\frac{i^E\cos б}{1+|\sin б|}д_1(c),$$

,

where

$$д_0(c) = \begin{cases} 1, c>1 \\ 1/2, c=1 \\ 0, c<1 \end{cases},\ д_1(c) = \frac{2}{\pi}\begin{cases} K(c), c<1 \\ \frac{1}{c}K\left(\frac{1}{c}\right), c>1 \end{cases}.$$

Connection between the components in case E is simplified:

$$S_n^x = \mathrm{tg}б\, S_n^y,$$

$$S_n^z = \frac{i^E}{2}\left[\left(S_{n-1}^y - S_{n+1}^y\right) + |2\mathrm{tg}б|\, N_n^E\right],$$

$$C_n^x = -\frac{i^E}{2}\left[\left(S_{n-1}^y + S_{n+1}^y\right) + \frac{2}{\cos б}N_n^E\right],$$

(10)

$$C_n^y = \frac{1}{2}\left(S_{n+1}^y\frac{1}{W_1^E(б)} - S_{n-1}^y W_1^E(б)\right),$$

$$C_n^z = \frac{i^E}{\cos б}S_n^y,\qquad R^x = -\frac{i^E\cos б}{1+|\sin б|}R^y,$$

$$R^z = -\frac{i^E\cos б}{1+|\sin б|}\frac{S_0^y}{2},$$

Integral M_n^E has been calculated in [6], N_n^E is similarly calculated for components $\bar{x}_x, \bar{x}_y$. For an azimuth average inductive velocity we obtain the final expressions:

$$\bar{x}_r^y = -\frac{k\bar{\Gamma}(\bar{r})}{4p\bar{v}},\qquad \bar{x}_r^x = -\frac{\mathrm{sgn}(б)\cos б}{1+|\sin б|}x_r^y,$$

$$\bar{x}_r^z = -\frac{k}{4p\bar{v}}\frac{\mathrm{sgn}(б)\cos б}{1+|\sin б|}\int_0^1\frac{d\bar{\Gamma}}{d\bar{c}}д_1(\tilde{c})d\bar{c},$$

If in Case E we take $\alpha=0$ (flat vortex sheet), harmonic connections are simplified and the x-th and the z-th components are expressed through the y-th component.

$$\bar{x}_{sn}^x = 0,\qquad \bar{x}_{sn}^z = -\frac{1}{2}\left[\bar{x}_{sn-1} - \bar{x}_{sn+1}\right]$$

$$\bar{x}_{cn}^y = -\bar{x}_{sn}^z,\qquad \bar{x}_{cn}^z = -\frac{\bar{v}}{\bar{r}}\bar{x}_{sn}^y,$$

$$\bar{x}_r^x = \bar{x}_r^y,\qquad \bar{x}_r^z = \frac{1}{2}S_0^y.$$

The second important case is Case L – calculation of inductive velocity from rotor flat vortex structure ($\alpha=0$). Here:

$$i^L = -\mathrm{sgn}(y),\quad W_n^L = \left(\frac{L-|y|}{l}\right)^n,\quad i^L y = -|y|$$

$$S_n^x = 0,\ S_n^y = M_n^L,$$

$$S_n^z = i^L\left[\frac{1}{2}\left(S_{n-1}^y - S_{n+1}^y\right) - |y| S_n^y\right],$$

$$C_n^x = -i^L\left[\frac{1}{2}\left(S_{n-1}^y + S_{n+1}^y\right) + N_n^L\right],$$

$$C_n^y = -i^L S_n^z,$$

$$C_n^z = i^L S_n^y,\ R^x = -i^L R^y,$$

$$R^y = д_0(c) + \frac{C_0^y}{2},\ R^z = i^L \frac{S_0^y}{2}$$

The components are also expressed through two typical integrals:

$$M_n^L = (-1)^{n+1}\frac{2}{\pi}\int_0^{\pi}\frac{\cos n\varphi}{L} W_n^L dИ,$$

$$N_n^L = (-1)^n \frac{2}{\pi}\int_0^{\pi} \cos n\varphi W_n^L dИ,$$

The relations between the harmonics are:

$$\bar{x}_r^x = -i^L \bar{x}_r^y, \qquad \bar{x}_{cn}^z = \frac{\bar{v}}{\bar{r}} i^L \bar{x}_{sn}^y,$$

$$\bar{x}_{cn}^y = -i^L \bar{x}_{sn}^z,$$

$$\bar{x}_{sn}^y = \frac{i^L}{2}\left[\left(\bar{x}_{sn-1}^y - \bar{x}_{sn+1}^y\right) - 2|y|\bar{x}_{sn}^y\right],$$

$$\bar{x}_r^z = \frac{1}{2}\bar{x}_{co}^z$$

Integrals M_n^L, N_n^L are reduced to a combination of polynoms and complete elliptic integrals of three genuses.

Case B – calculation of inductive velocity when the vortex sheet and the reference point are located at different disk sides ($y \sin\alpha \le 0$). Here

$$i^B = \text{const}, \quad W_n^B = W_n^E \cdot W_n^L$$

The variables also get separated

$$M_n^B = W_n^E M_n^L,\ N_n^B = W_n^E N_n^L$$

Equations of connection between the harmonics now look like:

$$R^x = -i^B W_1^E R^y,\ R^y = д_0(c) + \frac{C_0^y}{2},$$

$$R^z = i^B W_1^E \frac{S_0^y}{2}, \qquad S_n^x = \text{tg}б\, S_n^y, \quad S_n^y = M_n^B,$$

$$S_n^z = \frac{i^B}{2}\left[\left(S_{n-1}^y - S_{n+1}^y\right) + \frac{2|\sin б| N_n^B - |y| M_n^B}{\cos б}\right],$$

$$C_n^x = -\frac{i^B}{2}\left[\left(S_{n-1}^y + S_{n+1}^y\right) + 2\frac{N_n^B - |y \sin б| S_n^y}{\cos б}\right],$$

$$C_n^y = |y| S_n^y + \frac{1}{2\cos б} \times$$

$$\times\left[S_{n+1}^y - S_{n-1}^y + |\sin б| \times \left(S_{n+1}^y + S_{n-1}^y\right)\right]$$

$$C_n^z = \frac{i^B}{\cos б} S_n^y$$

In the general case of $y \sin\alpha > 0$ the inductive velocity components are expressed through four typical integrals. The integrals present combinations of algebraic functions and incomplete elliptic integrals of the 1st, 2nd and 3rd genuses [5].

Let us introduce functions

$$(11) \qquad ч^x\left(\bar{y}, \tilde{\Gamma}, б\right) = \frac{\bar{x}_c^x\left(\bar{y}, \tilde{\Gamma}, б\right)}{\bar{x}_c^x\left(\bar{y}=0, \tilde{\Gamma}, б\right)},$$

$$ч^y\left(\bar{y}, \tilde{\Gamma}, б\right) = \frac{\bar{x}_c^y\left(\bar{y}, \tilde{\Gamma}, б\right)}{\bar{x}_c^y\left(\bar{y}=0, \tilde{\Gamma}, б\right)},$$

as a ratio of an average inductive velocity in the plane located at $\bar{y}$ distance from the disk to eigen velocity at $\bar{y}$=0 for typical normalized circulation.

In fig. 2 and 3 these functions are presented. The graphs illustrate the velocity properties – in $y \cdot \sin\alpha \le 0$ domain velocities do not depend upon α. Zhukovsky theory ($\alpha = \frac{\pi}{2}$) correlates well with that of Vildgrube (α=0).

Vortex cylinder declination angles

In the plane of each coaxial rotor, besides eigen inductive velocity, there also exists an additional inductive velocity (fig.4).

For thrust coefficient $C_{Ty} = C_T^{UP} + C_T^{LO}$, $t_C = \frac{C_T^{LO}}{C_T^{UP}}$,

distances between the rotors $\bar{y}$*, vortex cylinder

declination angle α_1 and vortex shedding velocity V_1 we have a solving system

$$\begin{cases} \overline{V}_1^{UP}\cos\delta_1^{UP} = м^{UP} - \overline{x}_x^{UP} - \overline{x}_x^{UP\text{-}LO} = м_x^{UP} \\ \overline{V}_1^{LO}\cos\delta_1^{LO} = м^{LO} - \overline{x}_x^{LO} - \overline{x}_x^{LO\text{-}UP} = м_x^{LO} \\ \operatorname{tg}\delta_1^{UP} = \dfrac{\overline{V}_\infty \sin\delta_e^{UP} + \overline{x}_y^{UP} + \overline{x}_y^{UP\text{-}LO}}{\overline{x}_1^{UP}\cos\delta_1^{UP}} \\ \operatorname{tg}\delta_1^{LO} = \dfrac{\overline{V}_\infty \sin\delta_e^{LO} + \overline{x}_y^{LO} + \overline{x}_y^{LO\text{-}UP}}{\overline{x}_1^{LO}\cos\delta_1^{LO}} \end{cases}$$

where

$$м = \overline{V}_\infty \cos\delta_e$$

$$\overline{x}_y^{LO} = -\frac{C_{T\Sigma}}{4(1+t_C)\overline{V}_1^{LO}},\quad \overline{x}_y^{UP} = -\frac{C_{T\Sigma}t_C}{4(1+t_C)\overline{V}_1^{UP}},$$

$$\overline{x}_y^{LO\text{-}UP} = -\frac{C_{T\Sigma}t_C\, ч^y\left(-\overline{y}_*, \widetilde{\Gamma}_I, \delta_1^{UP}\right)}{4(1+t_C)\overline{V}_1^{UP}},$$

$$\overline{x}_y^{UP\text{-}LO} = -\frac{C_{T\Sigma}\, ч^y\left(\overline{y}_*, \widetilde{\Gamma}_I, \delta_1^{LO}\right)}{4(1+t_C)\overline{V}_1^{LO}},$$

$$\overline{x}_x^{LO} = \frac{C_{T\Sigma}\operatorname{sgn}\left(\delta_1^{LO}\right)k\left(\delta_1^{LO}\right)}{4(1+t_C)\overline{V}_1^{LO}}$$

$$\overline{x}_x^{UP} = \frac{C_{T\Sigma}t_C\operatorname{sgn}\left(\delta_1^{UP}\right)k\left(\delta_1^{UP}\right)}{4(1+t_C)\overline{V}_1^{UP}}$$

$$\overline{x}_x^{LO\text{-}UP} = -\frac{C_{T\Sigma}t_C\operatorname{sgn}\left(\delta_1^{UP}\right)k\left(\delta_1^{UP}\right)ч^X\left(-\overline{y}_*, \widetilde{\Gamma}_I, \delta_1^{UP}\right)}{4(1+t_C)\overline{V}_1^{UP}},$$

$$\overline{x}_x^{UP\text{-}LO} = -\frac{C_{T\Sigma}\operatorname{sgn}\left(\delta_1^{LO}\right)k\left(\delta_1^{LO}\right)ч^X\left(\overline{y}_*, \widetilde{\Gamma}_I, \delta_1^{LO}\right)}{4(1+t_C)\overline{V}_1^{LO}},$$

$$k(\delta) = \frac{-\cos(\delta)}{1+|\sin\delta|},$$ Solution of the system with respect to α_1 и V_1 is reached by the method of subsequent approximations and converges fast. Fig. (5) shows functions $\delta_1^{LO}, \delta_1^{UP} = f\left(V_\infty, \alpha_e\right)$.

For applications it is suitable to find an average angle for the lower rotor and the whole combination

$$\delta_C = \frac{\delta_1^{UP} + \delta_1^{LO}}{2}.$$

It is interesting to note that the declination angle for an equivalent single rotor considerably differs from α_c. There is an approximated formula for α_c:

$$\delta_C^\circ = \left(a_1 + a_2 C_T\right)\delta_e^\circ + \left(b_1 + b_2 C_T\right),$$

where

$$a_i = \sum_{n=0}^{n=4} a_{i\,n}\overline{v}^n, \quad b_i = \sum_{n=0}^{n=4} b_{i\,n}\overline{v}^n.$$

Solution of the task connected with the vortex cylinder declination angles is a part of the coaxial rotors mutual induction task.

Definition of circulation. To define average circulation along the blade section circumference, let us use designations of [6, page 52-53]. For a rotor operating in the field of alternating velocities, similar to formula 2.83 of [6] we can write:

$$\overline{\Gamma} = \frac{a_\infty \overline{b}}{2}\left\{\varphi_e \overline{r}\left(1 + \frac{м^2}{2\overline{r}^2}\right) + м[\operatorname{tg}\delta_{MR} + \Theta_{2e}] + \right.$$
$$\left. + \frac{1}{2\pi\overline{r}}\int_0^{2\pi}\left(\overline{x}_y^{eigen} + \overline{x}_y^{add}\right)\overline{W}d\text{ш}\right\}$$

where:

$$\varphi_e = \varphi_0 + Д\varphi - \overline{k}a_0,$$

$$И_{1e} = И_1 + \overline{k}a_1,\ И_{2e} = И_2 + \overline{k}b_1,$$

Assuming the additional velocity having been induced by the neighboring coaxial rotor of opposite sense of rotation we obtain a system of two integra-differential equations of coaxial rotor blade circulation that can be converted to the following

$$\overline{\Gamma}_q(\overline{r}) = B_q(\overline{r})\left\{\varphi_{e_q}\overline{r}\left(1 + \frac{м^2}{2\overline{r}^2}\right) + м[\operatorname{tg}\delta_{MR} + \Theta_{2e}]\right.$$
$$\left. - \frac{k}{4p\overline{v}_P}\int_{c_0}^{1}\overline{\Gamma}_P(\overline{c})K_{qP}\left(\overline{c}, \overline{r}, \overline{y}_q, \delta_{1P}\right)d\overline{c}\right\} \qquad (12)$$

$$q = 1,2 \qquad p = \begin{cases} 1, q = 2 \\ 2, q = 1 \end{cases},$$

where

$$B(\overline{r}) = \frac{a_\infty \overline{b}}{2 + \dfrac{ka_\infty\overline{b}}{4\pi\overline{V}}\left(1 + \dfrac{\mu^2}{\overline{r}^2}\cdot\dfrac{1}{1+|\sin\alpha_1|}\right)}$$

$$K_{qP}\left(\overline{c}, \overline{r}, \overline{y}_q, \delta_P\right) =$$

$$= \frac{d}{d\bar{c}}\left[I_{\Gamma}^{y}\left(\bar{c}, \bar{r}, (-1)^{q}\bar{y}_{*}, б_{1P} \right) - \frac{м}{2\bar{r}} I_{Sl}^{y}\left(\bar{c}, \bar{r}, (-1)^{q}\bar{y}_{*}, б_{1P} \right) \right]$$

Solution (12) is reduced to solution of linear algebraic equations system looking like $A \cdot \Gamma_q = C_q$. Using vector C_q decompensation to basic functions

$$C_q = \varphi_{0q} N_{\varphi}^{q}(r) + \varphi_{0P} N_{\varphi}^{qp} + \alpha_e N_{\alpha}^{q} + \alpha_e N_{\alpha}^{qp} + N_0^{q}$$

solution (12) can be conveniently sought in

$$(13) \qquad \bar{\Gamma}_q = \varphi_{0q}\bar{\Gamma}_{\varphi}^{q} + \varphi_{0P}\bar{\Gamma}_{\varphi}^{qp} + б_e\left(\bar{\Gamma}_{\alpha}^{q} + \bar{\Gamma}_{\alpha}^{qp} \right) + \bar{\Gamma}_0^{q}$$

where

$$\bar{\Gamma}_{\varphi}^{q} = A^{-1}N_{\varphi}^{q}, \bar{\Gamma}_{\varphi}^{qp} = A^{-1}N_{\varphi}^{qp}\bar{\Gamma}_{\alpha}^{q} = A^{-1}N_{\alpha}^{q},$$
$$\bar{\Gamma}_{\alpha}^{qp} = A^{-1}N_{\alpha}^{qp}, \bar{\Gamma}_0^{q} = A^{-1}N_0^{q},$$
$$q = 1,2$$

Through these functions and Fourier series expansion coefficients, inductive speed flap motion 1st harmonic coefficients are defined. Fig. 6,7 shows blade circulation and coaxial rotor flap motion coefficient functions.

If required, blade flap motion can be specified through numeric integration of blade flap differential equations.

At $y^{*}=\infty$ (12) are transformed to relations for a single rotor. Fig. 8 shows correlations of inductive velocity fields under the rotor obtained through calculations under (5), (12) and in Pavlov and Radchenko experiments.

Peculiarities of coaxial rotors in axial conditions. While for a single rotor inclusion of wake compression and vortex variation does not change the integral characteristics considerably, for coaxial rotors accounting for these factors becomes crucial.

To account for the vortex structure nonlinearity, functions of rotor wake compression and flow acceleration are introduced. For a single rotor these functions are easily obtained from the flow equation. For a coaxial rotor the lower rotor vortex structure follows that of the upper rotor equidistantly from y* to ∞.

The calculation method for coaxial rotor aerodynamic characteristics in axial conditions including the flow compression has been developed at Kamov Company by V. A. Anikin and is described in [7] where there are also presented coefficients of correction offered by V.N. Kvokov for tuning the model for flight tests. As shown by the experience of coaxial rotor analysis program practical application, these coefficients are not required in the majority of cases and the mathematical model gives satisfactory results both for single and coaxial rotors. Fig. 9 shows coaxial rotor drag polars based on analytical and experimental results obtained by V. F. Antropov. At fig. 10 single rotor drag polars obtained at Kamov Company through experiment and analysis are presented.

Calculation of the main rotor system forces and moments. When defining the coaxial main rotor forces and moments integration of all known relations for elementary rotor forces and moments [ ] with consideration to re-distribution of angles of attack in the blade sections caused by additional inductive flow from the neighboring rotor vortex system and changes of the blade flap motion is used:

$$(14) \quad \begin{aligned} C_T &= \frac{k}{2\pi^2}\int_0^{2\pi}\int_0^1 \bar{b}\bar{W}_1^2\left(C_y \cos в_1 + C_{xp}\sin в_1 \right) d\bar{r}dш \\ C_H &= \frac{k}{2\pi^2}\int_0^{2\pi}\int_0^1 \bar{b}\bar{W}_1^2[\left(C_{xp}\cos в_1 - C_y \sin в_1 \right)\sin ш \\ &\quad - \left(C_y \cos в_1 + C_{xp}\sin в_1 \right)\cos ш \sin\beta]d\bar{r}dш \\ m_K &= \frac{k}{2\pi^2}\int_0^{2\pi}\int_0^1 \bar{r}\bar{b}\bar{W}_1^2\left(C_{xp}\cos в_1 - C_y \sin в_1 \right)\times \\ &\quad \times \cos\beta d\bar{r}d\psi \end{aligned}$$

To define Cy and Cxp a flat section hypothesis was used along with the blade profile characteristics obtained in ADT tests.

The rotor aerodynamic analysis is divided into two parts: 1) definition of vortex cylinder inclination angles, circulation, blade flap motion and inductive velocity field; 2) calculation of forces and moments and, if required, specification of blade flap motion.

For the angle of attack in the blade section we have [6, page 53]:

$$б = \varphi(r) - \bar{k}в + \varphi_{y\ p}(ш) + \arctan\frac{\bar{V}\sin б_B + \bar{x}_{y_y} - \left(\bar{r}\frac{dв}{dш} + м\cos ш \right)}{\bar{W}_*}$$

For inductive speeds in each rotor lane we have (5), (12):

$$x_y^{q}(\bar{r}, ш) + x_y^{qp}(\bar{r}, ш)$$

As a result, using experimentally obtained relations $C_y = f(б, M, Re), C_{xp} = f(б, M, Re)$ we can define elementary forces $C_y(r, ш)$, $C_{xp}(r, ш)$ in each section $(r, ш)$ and further under (14) the rotor forces and moments.

Calculation of forces and moments on the airframe. To calculate forces and moments on the airframe the results obtained in the ADT tests of an airframe model are used. To recalculate the airframe element parameters to full scale parameters and to account for the influence caused by the main rotor system, formulas (5) for all inductive velocity components are used. Besides, in the angles of attack of the i-th airframe element a wash from the rotor rotation is accounted for through $Дб = \frac{ш_z}{v} x_i + \frac{ш_y}{v} z_i$.

Definition of δ_z, realized on the aircraft $M_Z=0$ is performed according to a subsequent approximation pattern.

Results of modeling. A large experience in modeling has been accumulated during long standing application of aircraft characteristics analysis programs. The created mathematical model ensures an acceptable level of accuracy and is well applicable for solution of a wide range of application tasks. Figs. 11-17 show comparison of coaxial helicopter main flight characteristics obtained in flight tests and by analysis. Fig. 11 shows required power, fig. 13 – drag polar at hover. Figs. 14-16 show balance relations in horizontal flight, at climb and descent and fig. 17 – the same for tail forward flight. The analytical and experimental data correlate well.

References

1. В.А. Аникин. Дисковая вихревая теория винта и ее приложения в а родинамике вертолетов. Труды вторых научных чтений, посвященных памяти акад. Б.Н.Юрьева, Москва, 23-24 марта 1987 г., ИИЕТ АН СССР, М., 1988 г.

2. В.А. Аникин, Б.А. Васильев. Метод расчета балансировки соосного вертолета на начальных стадиях проектирования. В сб. « роблемы проектирования вертолетов народнохозяйственного применения», М., МАИ, 1986 г.

3. В.А. Аникин. К теории индукции несущего винта вертолета. В сб. «Вопросы конструкции и проектирования самолетов», Таш И, Ташкент, 1981 г.

4. В.А. Аникин. К вихревой теории несущего винта. Изд. АН СССР, МЖСГ, 1982 г., № 5, с. 169-172.

5. В.А. Аникин. О свойствах индуктивных скоростей несущего винта. В сб. «Научно-методические материалы по прикладным задачам а ромеханики"», ХАИ, Харьков, 1986 г.

6. В. . Баскин, Л.С. Вильдгрубе, Е.С. Вождаев, Г.И. Майкапар. Теория несущего винта. М., Машиностроение, 1973 г.

   Baskin V.E., Vildgrube L.S., Vozgdayev Ye.S., Maykapar G.I., Theory of the Lifting Airsqrew. NASA TT F-823, 1976.

7. V.N. Kvokov. Factor analysis of coaxial rotor aerodynamics in hover/ Forum Proceedings of the 18th European Rotorcraft Forum, 1992.

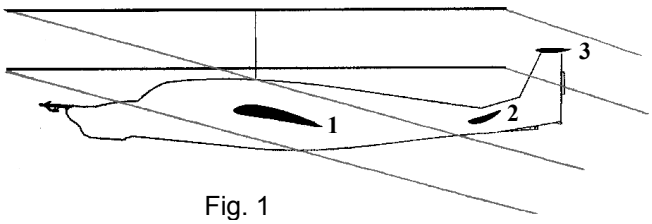

Fig. 1

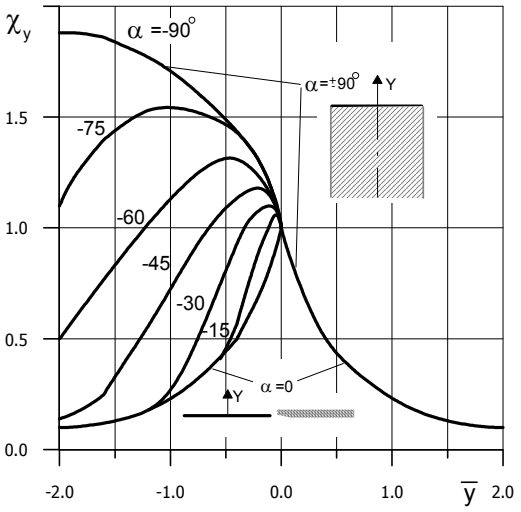

Fig. 2

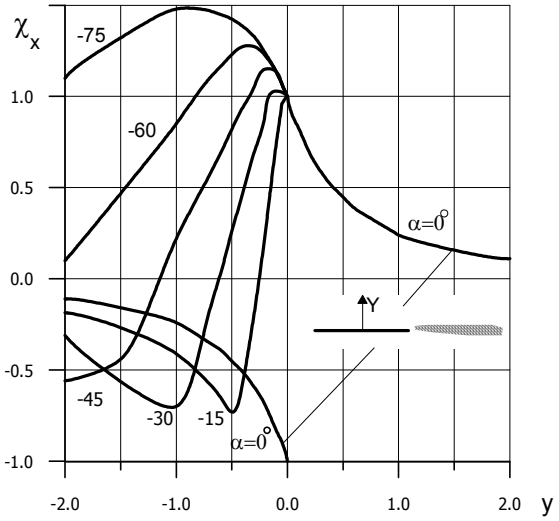

Fig. 3

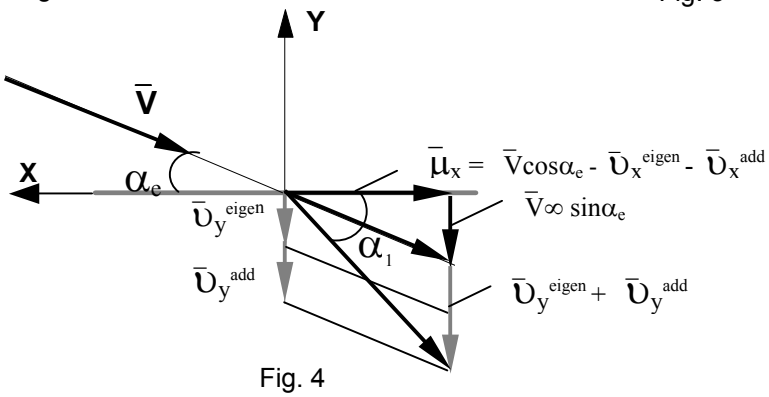

Fig. 4

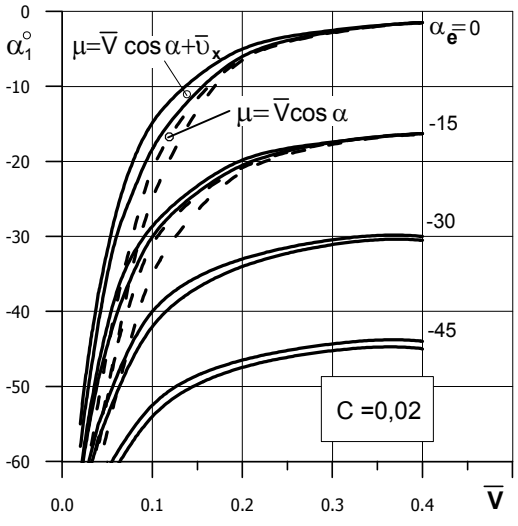

Fig.5 Coaxial rotor vortex cylinder deflection angel

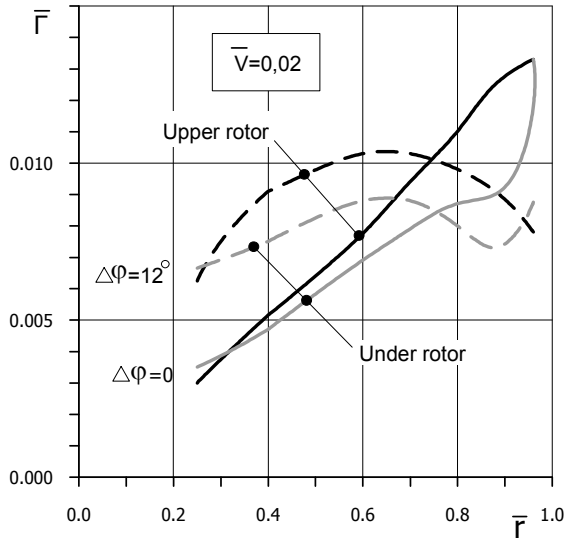

Fig.6 Blade span flow circulation for upper and lower coaxial rotors

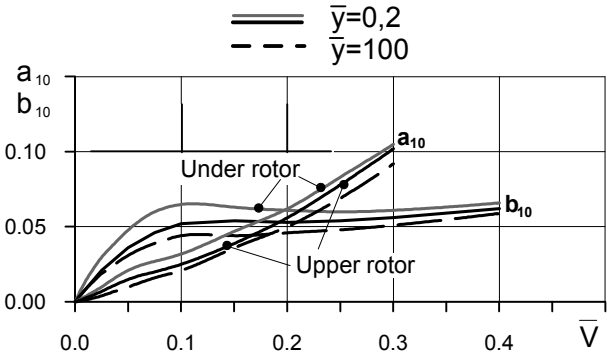

Fig.7 1st harmonic flapping coefficients

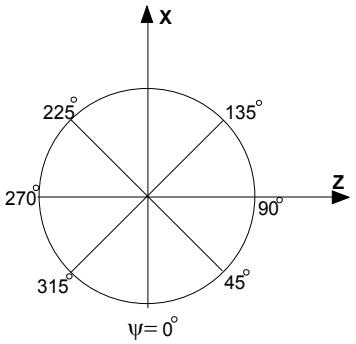

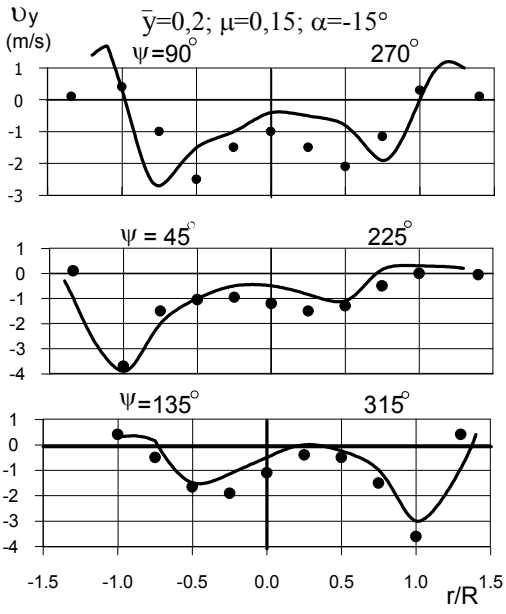

Fig.8 Induced velocity in in the main rotor plane (single rotor)

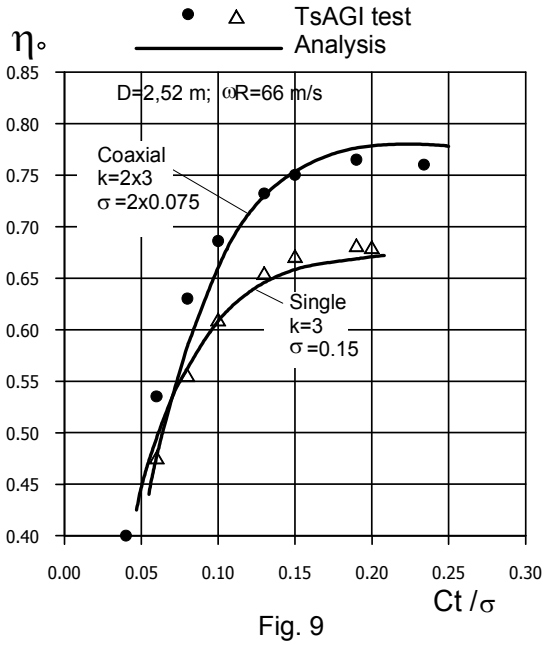

Fig. 9

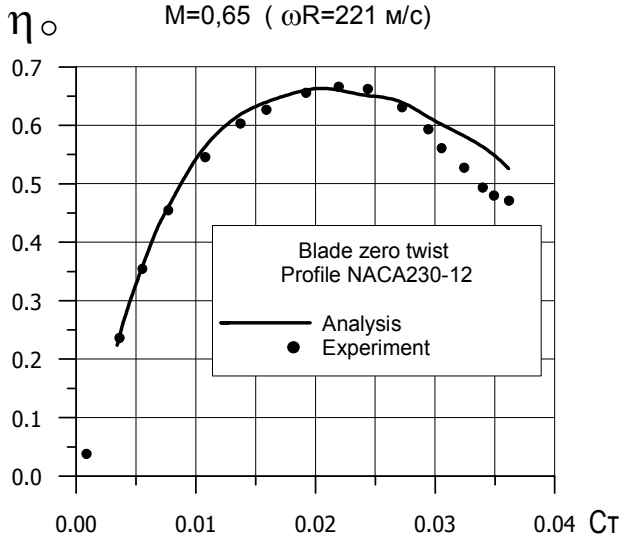

Fig. 10

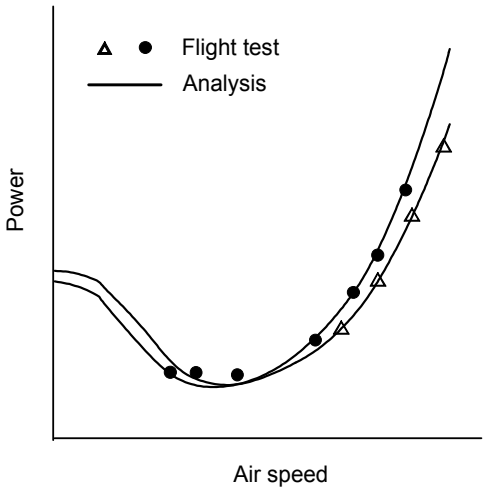

Fig.11 Coaxial helicopter required power in level flight

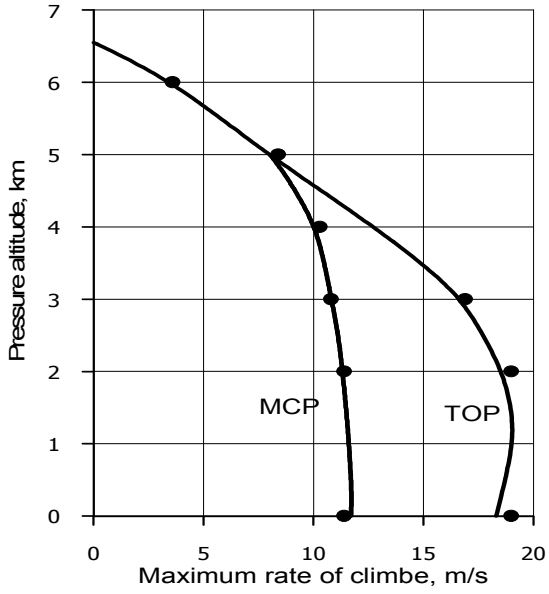

Fig.12

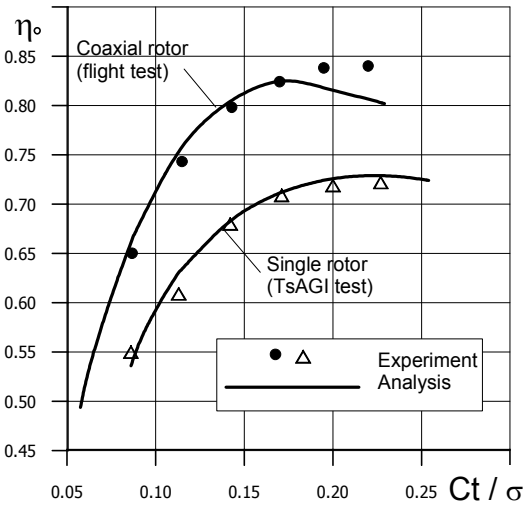

Fig 13

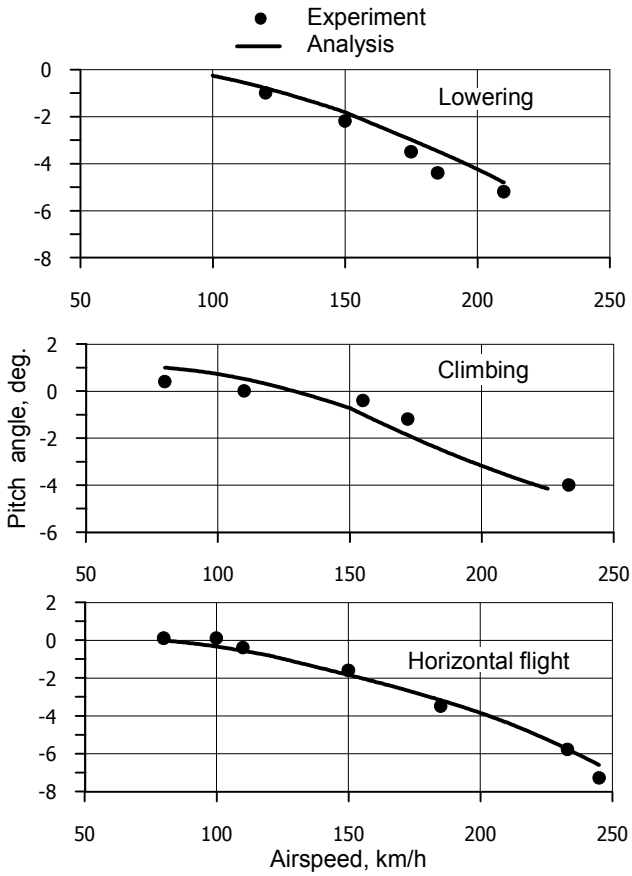

Fig.14 Helicopter pitch angle vs airspeed

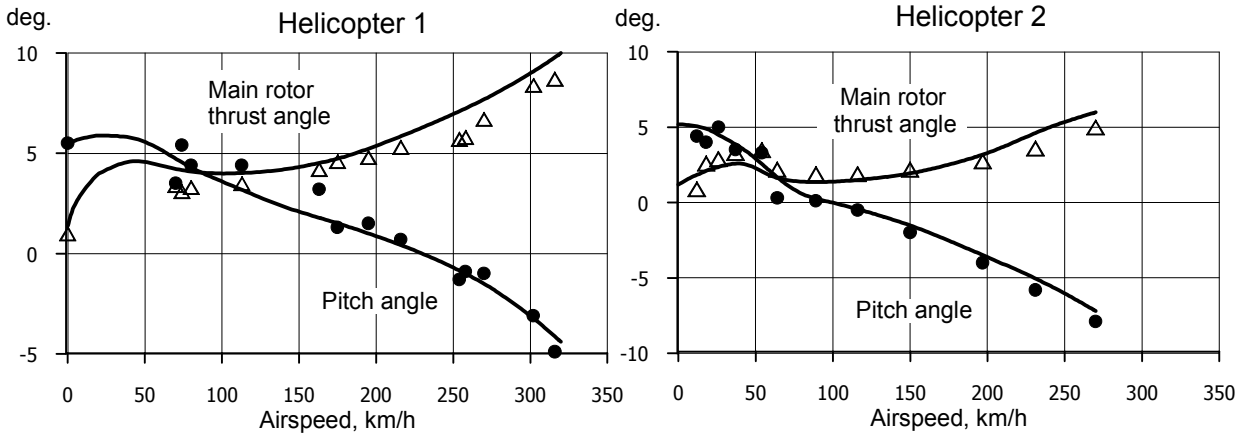

Fig. 15

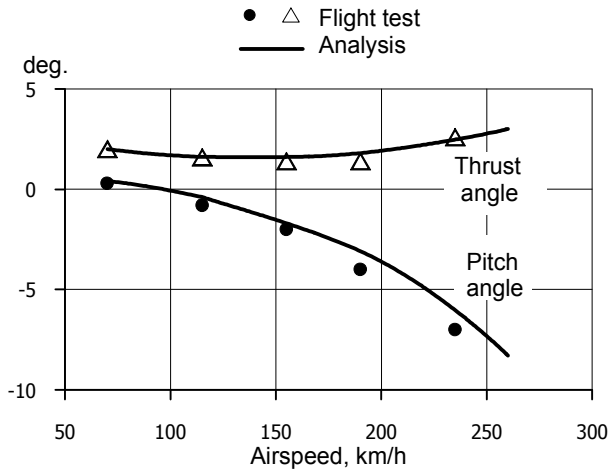

Fig.16 Lowering, V_Y=-5 m/s

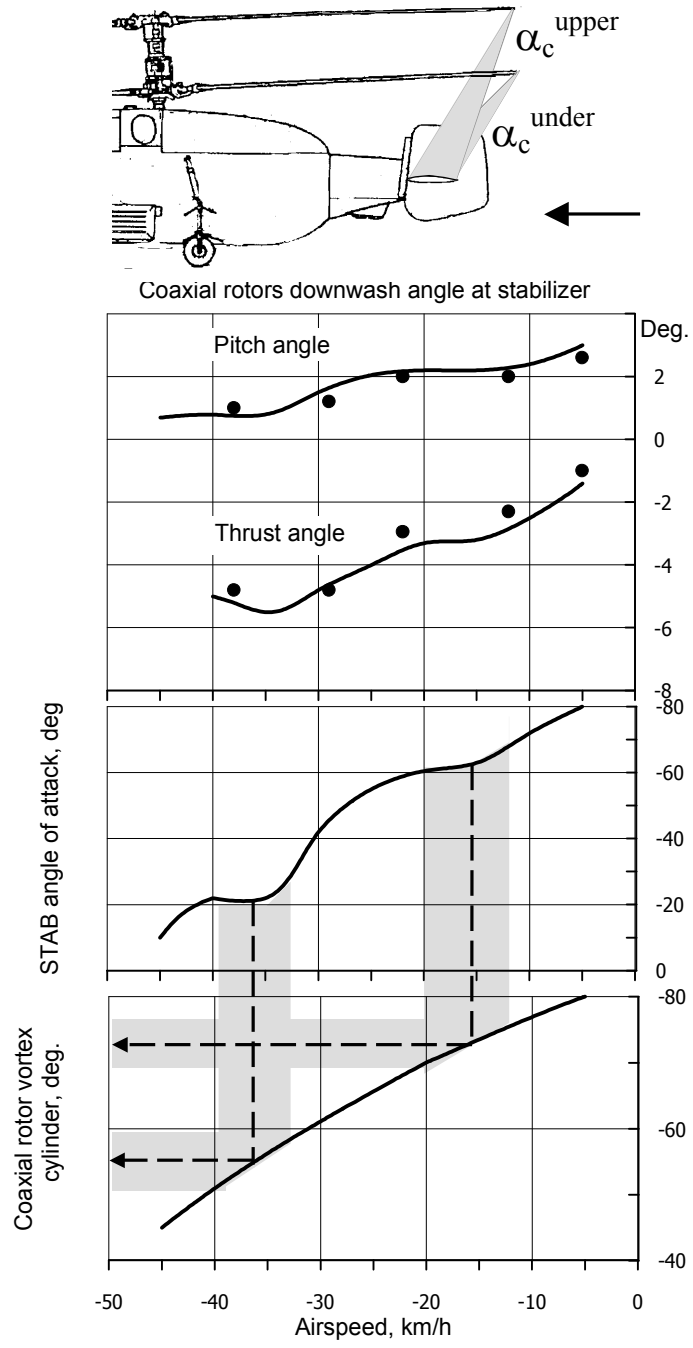

Fig.17 Helicopter back flight